Progress In Electromagnetics Research B, Vol. 97, 115–130, 2022

An Optimization Analytical Method for Synchronous Machine Model Design from Operational Inductance *Ld(s)*

Farid Leguebedj*, Djamel Boukhetala, and Mohamed Tadjine

Abstract—This paper presents an analytical method for the optimal estimation of time constants of synchronous machine from Stand Still Frequency Response Testing (SSFR). We show that the analytical method is advantageous over the conventional one since the latter is based on curve fitting representing the variation of the operational inductance as a function of the frequency and provides inaccurate and non-unique solutions. In fact, the analytical method applies the standard theory of linear systems to locate the values of poles and zeros in the frequency response and determines the optimal order of the equivalent circuit that can model the machine accurately. The proposed method is simple, practicable, and effective. However, it needs an optimisation process based on parameter differentiation to improve the values of time constants. Based on the measured data, realistic tests are given to show the advantages of the method.

List of Symbols

s: Laplace's operator
Vd: d-axis stator voltage
Vf: d-axis field voltage
$Zd(s)$: d-axis operational impedance
$Ld(s)$: d-axis operational inductance
Ld: d-axis synchronous inductance
Ra, Rf: armature and field resistances
Rk, Rb, Re: d-axis damper resistances
Lk, Lb, Le: d-axis magnetizing inductance
Lmd: direct-axis armature to rotor mutual inductance
$Lamd$: the parallel combination of Lmd and La
$Lamdf$: the parallel combination of Lmd, Lf and La
$Lmdf$: the parallel combination of Lmd and Lf
$Td0'$, Td': d-axis transient open circuit and short-circuit time constant
$Td0''$, Td'': d-axis subtransient open circuit and short-circuit time constant
$Td0'''$, Td''': d-axis sub-subtransient open circuit and short-circuit time constant
$Td0''''$, Td'''': d-axis sub-sub-subtransient open circuit and short-circuit time constant
Fce: center frequency
β: constant

Received 1 July 2022, Accepted 4 November 2022, Scheduled 24 November 2022
* Corresponding author: Farid Leguebedj (farid.leguebedj@g.enp.edu.dz).
The authors are with the Process Control Laboratory, Automatic Control Department, 10 Avenue H. Badi BP 182, ENP Alger, Algeria.

1. INTRODUCTION

Synchronous generators are the most important parts of a supply system. Analysis of the behavior of synchronous generators for studying the stability and power control requires the knowledge of the parameters of synchronous machine [1]. The accurate identification of these parameters is very important. Several measurement techniques and identification methods have been reported in the literature for the determination of synchronous machine model parameters [2]. The graphical analysis of short-circuit tests [3, 4] is a classic of the IEEE standard 115 [5] allowing to obtain the parameters of d-axis and cannot identify the parameters of q-axis. Some investigations [6–8] based on the time analysis of the machine's response to standstill (Standstill Time Response or SSTR) have been examined. A similar approach with a rotating rotor (Rotating Time-Domain Response or RTDR) is described in the IEEE standard 115 [5]. RTDR has been used to determine machine parameters along both axes [9, 10].

The rapid development of computers has allowed the emergence of several other identification methods for the model of a synchronous generator. Indeed, it is possible to estimate parameters during normal operation of the machine (On-line measurements). Such methods are classified into two categories. The first is based on a "grey box" modeling in which we assume a known model structure such as the use of orthogonal series [11, 12] or the use of Kalman filter [13]. The second uses a "black box" modeling in which no model structure is assumed to be known a priori. In this case, the only objective of the identification is to establish the correspondence of the inputs to the outputs of the system using the method of neural networks [14, 15] or Volterra series [16].

Currently the most widespread approach for determining the parameters of the d-q model from SSFR stand still frequency response test has been introduced in [17]. During the SSFR frequency tests at standstill, the machine is stationary, and the rotor is aligned along the d-axis or q-axis. Two phases of the stator are supplied in series by a sinusoidal voltage source of variable frequency. The machine parameters are then determined by a transfer function optimization process characterizing the d-q model.

Despite the popularity of SSFR, only some publications [18] present the experimental setup in detail (for example the technical characteristics of the measuring and recording devices, the range and number of frequencies tested, the magnitude of source voltage). Such information is necessary to obtaining satisfactory measurements for data analysis. Some authors have investigated issues that can affect SSFR results, including the level of machine magnetization during testing [19, 20] and variation in stator resistance [21].

Apart from these experimental considerations, another difficulty of the SSFR method concerns the identification of the parameters from the measured data. Indeed, as in any problem of identification of a system, it is necessary to choose the type of model, estimator, the algorithm of minimization, and the initial values to be imposed. The different possible structures of the d-q model are presented in the IEEE standard 1110 [22]. The variants mainly depend on the number of branches used to represent the rotor circuit in each axis according to the type of construction of the rotor [23].

Regarding the identification method used, the method suggested in the IEEE standard 115 [5] is the method of least squares. It consists in minimizing the weighted sum of the errors between the transfer functions predicted by the chosen model and those measured experimentally. This method is straightforward and easy to implement using the Levenberg-Marquardt and Gauss-Newton algorithms. A major drawback of this method is that the result can converge to a local minimum depending on the initial values used and the choice of model. Other more robust alternatives are presented in some publications, such as the Maximum Likelihood Method [24], genetic algorithms [25, 26], and particle swarm optimization [27], or stochastic fractal search algorithm [28]. However, their implementation is more complex and requires more computing power than the methods suggested in the IEEE 115 standard [5].

In this paper, the results of the time constants estimation of synchronous machine from Standstill Frequency Response Testing (SSFR) are presented. An efficient identification method is used for optimal estimation of the time constant based in differentiation of frequency, magnitude, phase, and slope, and directly determines the exact order of the model representing the equivalent circuits. This analytical method is applied to real data, and the results are very satisfactory.

2. DIRECT-AXIS MODEL STRUCTURE OF A SYNCHRONOUS MACHINE AND PARAMETERS

The determination of synchronous machine parameters from the transfer function represents the operational inductance as a function of frequency. The operational inductance is derived from the machine's impedance which is measured at the terminals of the stator. This method has three main steps:

- Conversion of impedance to the operational inductance.
- Determination of the time constants from the operational inductance.
- Determination of machine's parameters from inductances and time constants.

The conversion of the machine's impedance to the operational inductance is based on the equivalent circuit of the direct axis of a synchronous machine used for the transient studies, Figure 1.

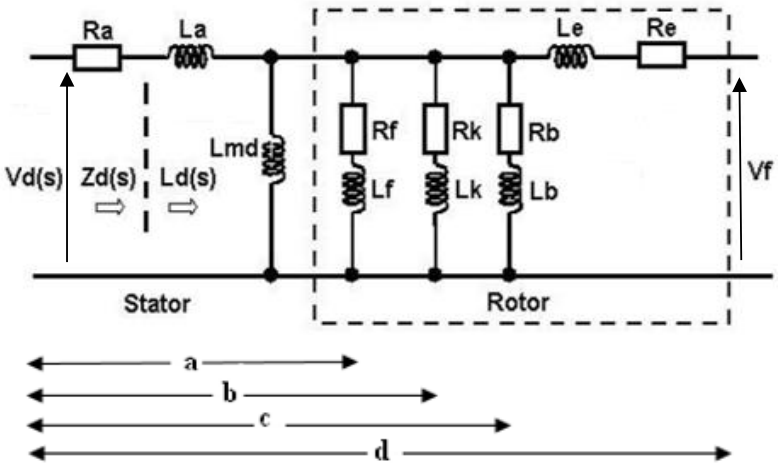

Figure 1. Equivalent Circuit of a fourth order model for direct axis.

2.1. Analysis of Synchronous Machine Models

2.1.1. First Order Model

Figure 1(a) shows the equivalent circuit for the first order model, and the $Ld(s)$ of this circuit is calculated as below [29]:

$$Ld(s) = \frac{Rf\,(La + Lmd) + s(LaLmd + LaLf + LmdLf)}{Rf + s(Lmd + Lf)} \tag{1}$$

Equation (1) can be written in standard form as follows:

$$Ld(s) \;=\; Ld\frac{(1 + sTd')}{(1 + sTd0')} \tag{2}$$

$$Ld \;=\; La + Lmd \tag{3}$$

2.1.2. Second Order Model

Figure 1(b) represents the derivation of the operational inductance of the second order model. The operational inductance of this model can be written as [29]:

$$Ld(s) = \frac{(La + Lmd)\,(Rf + sLf)\,(Rk + sLk) + sLaLmd(Rf + sLf + Rk + sLk)}{(Rf + sLf)\,(Rk + sLk) + sLmd(Rf + sLf + Rk + sLk)} \tag{4}$$

Equation (4) can be simplified, giving:

$$Ld(s) = (La + Lmd)\frac{1 + s\left[\frac{Lf + Lamd}{Rf} + \frac{Lk+Lamd}{Rk}\right] + \frac{s^2\,(LfLk + Lamd)\,(Lk + Lamdf)}{RfRk}}{1 + s\left(\frac{Lf + Lmd}{Rf} + \frac{Lk + Lmd}{Rk}\right) + \frac{s^2\,(Lmd + Lf)\,(Lk + Lmdf)}{RfRk}} \tag{5}$$

Equation (5) of the operational inductance becomes:

$$Ld(s) = Ld\frac{\left(1 + s\,(Td' + T1) + s^2 Td'Td''\right)}{(1 + s\,(Td0' + T2) + s^2 Td0'Td0'')} \tag{6}$$

where:

$$\begin{aligned} T1 &= (Lk + Lamd)/Rk; \\ T2 &= (Lk + Lmd)/Rk \end{aligned} \tag{7}$$

Applying the quadratic formula for the numerator and denominator of $Ld(s)$, we obtain the roots of the zero-pole extracted from Equation (6), and it has been proven that the roots of the last equation are real whatever the time constants. Hence the operational inductance for a second order model can be written as:

$$Ld(s) = Ld\frac{(1 + sTd')\,(1 + sTd'')}{(1 + sTd0')\,(1 + sTd0'')} \tag{8}$$

2.1.3. Third Order Model

Using the derivation method described above, the transfer function of the operational inductance for a model of the third order shown in Figure 1(c) can be expressed by:

$$Ld(s) = Ld\frac{(1 + sTd')\,(1 + sTd'')\,(1 + sTd''')}{(1 + sTd0')\,(1 + sTd0'')\,(1 + sTd0''')} \tag{9}$$

2.1.4. Fourth Order Model

The equivalent circuit for the fourth order model is shown in Figure 1(d). It is clear from previous analysis that a pair of poles zeros are added in each transfer function.

The operational inductance is given by:

$$Ld\,(s) = Ld\frac{(1 + sTd')\,(1 + sTd'')\,(1 + sTd''')\,(1 + sTd'''')}{(1 + sTd0')\,(1 + sTd0'')\,(1 + sTd0''')\,(1 + sTd0'''')} \tag{10}$$

3. EXPERIMENTAL TESTS ON A PRODUCTION GENERATOR

In order to validate the method used, we choose a machine of power 277.8 MVA and voltage 16.5 KV. The SSFR results are published in the work EPRI [30], and the d-axis impedance has been introduced for the determination process of synchronous machine model and time constants.

4. THE OPERATIONAL INDUCTANCE

In order to explain the procedure of determination of a frequency response of $Ld(s)$, we use the experimental measurements of the impedance $Zd(s)$ given in [30], Figure 2.

Equation (11) gives the expression of $Ld(s)$:

$$Ld\,(s) = \frac{Zd(s) - Ra}{s} \tag{11}$$

The stator resistance Ra is expressed by:

$$Ra = \lim_{s\to 0} |Zd(s)| \tag{12}$$

The principle of the method for measuring the armature resistance consists in considering the asymptotic value (for frequency approaching zero) of the real part of the operational impedance. The measured data was extrapolated using MATLAB's Curve Fitting. The curve fitting was done using the polynomial fitting option. The polynomial degree is chosen so as to have the best R-squared value. For this, a 4th order polynomial fit, Figure 3, provides the value of $Ra = 0.002000\,\Omega$.

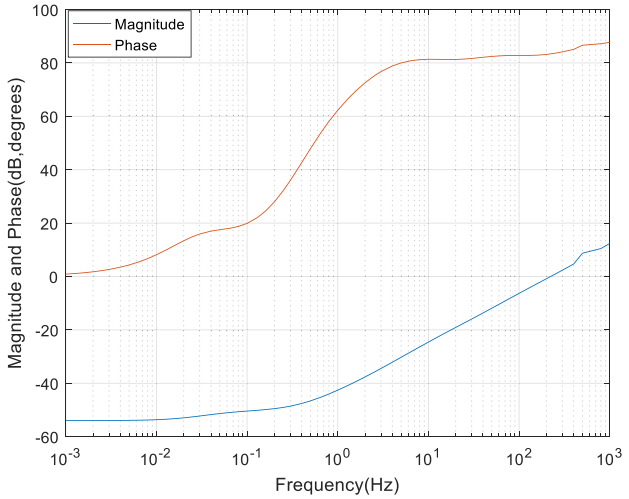

Figure 2. Frequency response of the impedance (measured data).

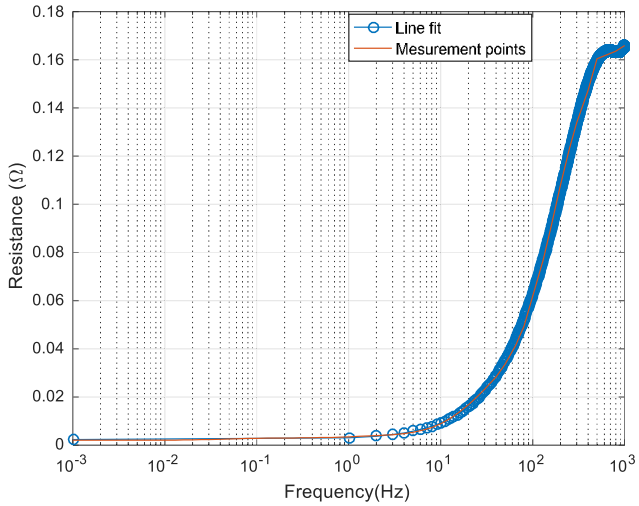

Figure 3. Variation of the resistance versus frequency.

Figure 4 shows the magnitude of the operational inductance in Henry [H] as function of frequency. When the frequency tends to zero, the asymptotic value of $|Ld(s)|$ represents the value of synchronous inductance $Ld = 0.004898\,\mathrm{H}$.

Figure 5 illustrates the operational inductance magnitude in dB and its phase in degree as function of frequency.

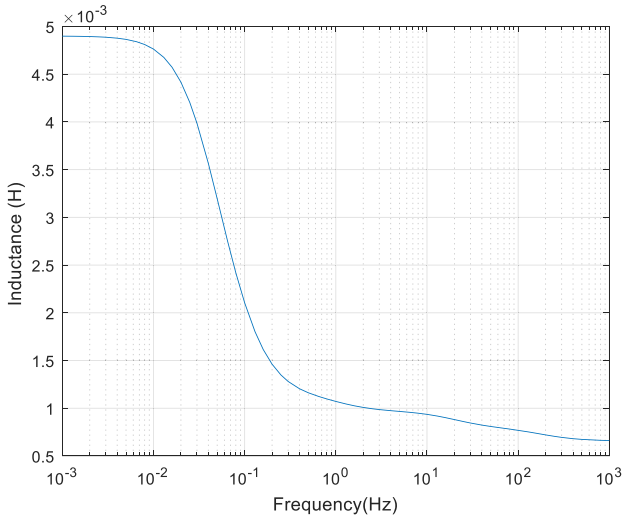

Figure 4. Variation of the operational inductance (in H) versus frequency.

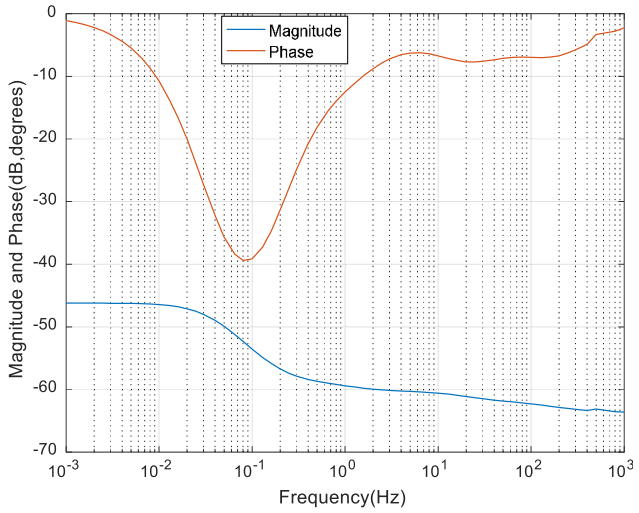

Figure 5. Frequency response of the operational inductance in terms of magnitude (in dB) and phase in (degrees).

5. SENSITIVITY TO STATOR RESISTANCE

In this section, we analyse the effect of the the stator resistance on the operational inductance in terms of magnitude and phase. For this, several stator resistances have been considered, as follows:

$$Ra - 2\%Ra, \quad Ra - 4\%Ra, Ra, \quad Ra + 2\%Ra \quad \text{and} \quad Ra + 4\%Ra$$

Note that $Ra = 0.00200\,\Omega$.

Figure 6(a) (respectively 6(b)) shows the evolution of the operational inductance magnitude (respectively phase) versus frequency for different stator resistances. We notice that there is a significant difference in the phases and magnitudes of the operational inductance at the beginning of the frequency. The difference between the curves decreases as the frequency increases. The values of the phases as well as the magnitudes begin to coincide from the 0.08 Hz frequency. For this frequency, all phase curves pass through a minimum. The difference between them does not exceed 6 degrees. Such difference still decreases with the frequency increase. Beyond 1 Hz, a total coincidence among all curves is observed.

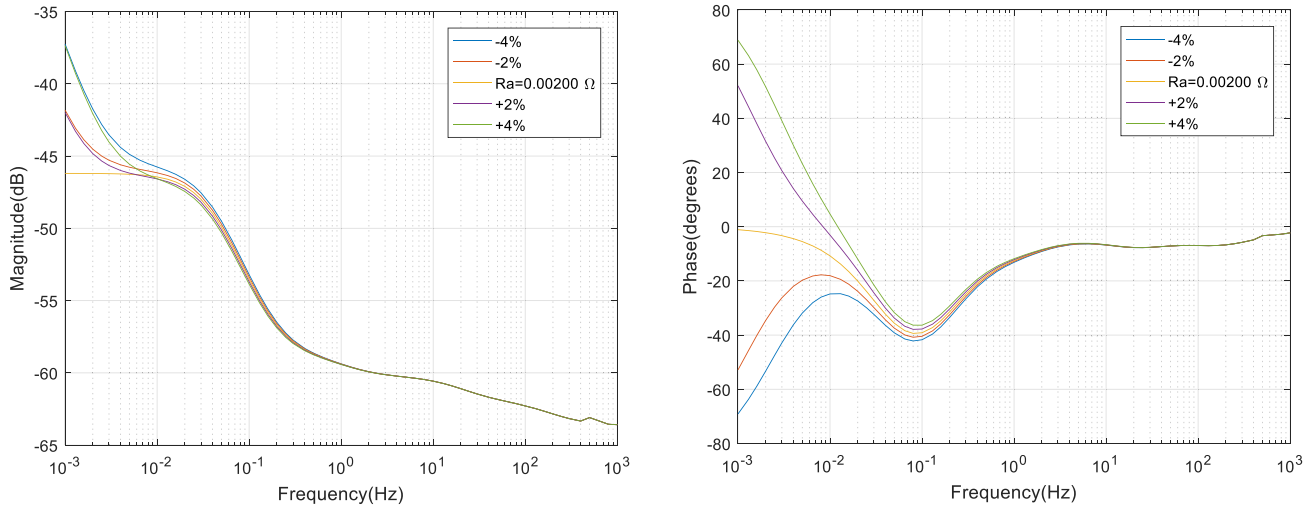

(a) (b)

Figure 6. (a) Frequency response of the operational inductance magnitude, for different stator resistances. (b) Frequency response of the operational inductance phase, for different stator resistances.

In our study, we have interested in the minimum highlighting by the phase curves for 0.08 Hz, since such minimum is paramount in the determination of the initial time constants, using the analytical method.

6. TIMES CONSTANT DETERMINATION

It is this part of the process that is most crucial for determining the parameters of the machine, since the values of the resistances and inductances of the branches of the equivalent circuit are intimately linked to these time constants.

6.1. Numerical Curve Fitting Techniques

Numerical curve fitting techniques were used to find the best time constants to fit the frequency response data employing the magnitude and phase of the measured data. This process has several problems such as:

- Before beginning the analysis, we predefine the model's order.

- Fit the curve, with an initial estimate of parameters.
- Define a cost function for optimising.

By using the commands 'freqs' and 'invfreqs' in MATLAB, we can convert the measured data of frequency response to transfer function for different models.

The following results have been obtained with MATLAB.

First order model:

$$Ld(s) = 0.004500\frac{(1 + 0.491032s)}{(1 + 2.301883)} \tag{13}$$

Second order model:

$$Ld(s) = 0.004898\frac{(1 + 0.820584s)\,(1 + 0.005902s)}{(1 + 3.858375s)\,(1 + 0.008495s)} \tag{14}$$

Third order model:

$$Ld(s) = 0.004899\frac{(1 + 0.896976s)\,(1 + 0.084855s)\,(1 + 0.002473s)}{(1 + 3.944719s)\,(1 + 0.101208s)\,(1 + 0.003354s)} \tag{15}$$

6.2. The Analytical Method

The analytical method is based on the standard theory of linear systems. Otherwise, the equivalent circuits of the synchronous machine are formed by simple branches (R, L), connected in parallel. So, these branches can be represented in the complex plane by a series of pairs poles-zero combinations. With this, it is possible to separate the transfer function by applying iterative subtraction of individual frequency responses for the particular branch. In a pole-zero the center frequency corresponds to the point with minimum phase. As a consequence, a parameter beta can be defined, related to both the value phi of the minimum phase and the gain change Gch of the pole-zero pair:

$$\sin(\varphi) = \frac{1 - \beta}{1 + \beta} \tag{16}$$

$$Gch = -20\log_{10}(\beta)\ (\text{dB}) \tag{17}$$

The values of time constants Td and $Td0$ can then be obtained from:

$$Td = \frac{\sqrt{\beta}}{2\pi Fce} \tag{18}$$

$$Td = \frac{Td0}{\beta} \tag{19}$$

In order to identify the time constants, the analytical method begins with the first identification of pole-zero pair from the operational inductance shown in Figure 5. The subtraction of the frequency response of the operational inductance gives a new residue frequency response. From this, the other pole-zero pair is identified from the next minimum phase. The substraction of the frequency responses of successive pole-zero pairs is done until there are no peaks of phase. The process is finished, and the model order is finally determined.

To implement the analytical method we propose the following steps:

- Step 1: first pole-zero pair
  According to Figure 5, the minimum phase of the operational inductance data $\varphi_{\min} = -39.37$ degree corresponds to the center frequency $Fce = 0.08$ Hz. Using Equation (16), we find $\beta = 4.4693$, and by Equations (18) and (19), respectively, we get $Td0'(\text{sec}) = 4.207969$, $Td'(\text{sec}) = 0.941527$, where $Td0'$ is the first pole, and Td' is the first zero.

$$H1(s) = \frac{(1 + sTd')}{(1 + sTd0')} \tag{20}$$

  is the transfer function of the 1st pole-zero pair.

- Step 2: second pole-zero pair
  We define Error1 as follows:

$$Error1_{magnitude} = |Ld(s)| + 46,1991 - 20\log_{10}|H1(s)| \tag{21a}$$
$$Error1_{phase} = Phase_{Ld(s)} - Arg(H1(s)) \tag{21b}$$

  where $Ld(s)$ is operational inductance (measured data).
  The variation of Error1 as a function of frequency is shown in Figure 7(a).
  The first minimum phase $\varphi_{\min} = -5.211$ degrees, which corresponds to the center frequency $Fce = 1.3\,\text{Hz}$, then $\beta = 1.1997$, $Td''(\text{sec}) = 0.111834$, $Td0''(\text{sec}) = 0.134168$, where $Td0''$ is the second pole, and Td'' is the second zero.

$$H2(s) = \frac{(1 + sTd'')}{(1 + sTd0'')} \tag{22}$$

  is the transfer function of the 2nd pole-zero pair.
- Step 3: third pole-zero pair
  Error2 is defined as follows:

$$Error2_{magnitude} = |Ld(s)| + 46,1991 - 20\log_{10}|H1(s)H2(s)| \tag{23a}$$
$$Error2_{phase} = Phase_{Ld(s)} - Arg(H1(s)H2(s)) \tag{23b}$$

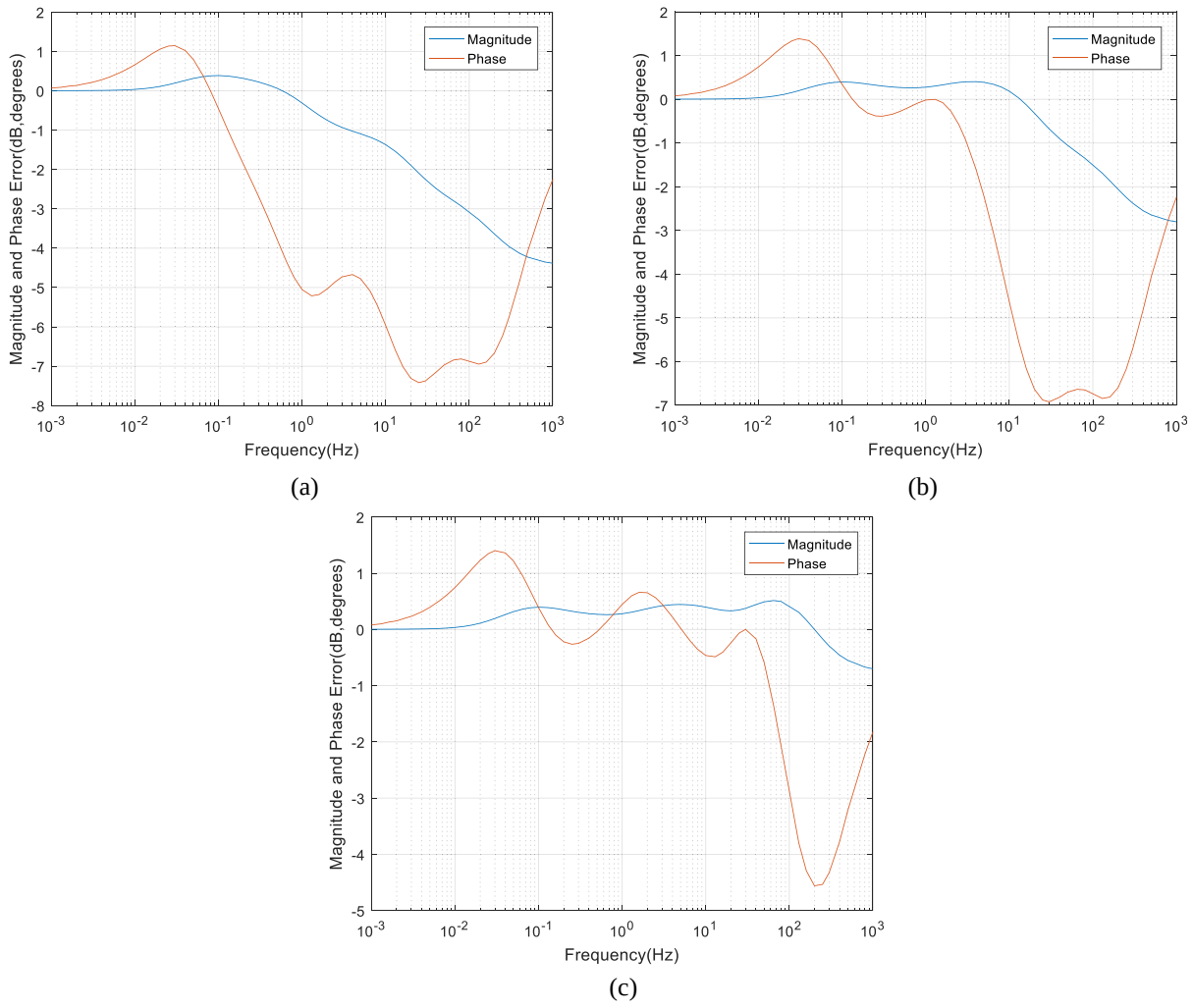

Figure 7. (a) Variation of magnitude and phase Error1 versus frequency. (b) Variation of magnitude and phase Error2 versus frequency. (c) Variation of magnitude and phase Error3 versus frequency.

Figure 7(b) represents the variation of the magnitude and the phase of the error2 according to the frequency.

We find that the first minimum phase corresponds to the value $\varphi_{\min} = -6.92$ degree, with $Fce = 30\,\text{Hz}$. By applying Equations (16), (18), and (19), we find: $\beta = 1,2740$, $Td'''(\text{sec}) = 0.0047025$, $Td0'''(\text{sec}) = 0.0059910$, where $Td0'''$ is the third pole, and Td''' is the third zero.

$$H3(s) = \frac{(1 + sTd''')}{(1 + sTd0''')} \tag{24}$$

is the transfer function of the 3rd pole-zero pair.

- Step 4: fourth pole-zero pair
  We calculate Error3 in the following way:

$$Error3_{magnitude} = |Ld(s)| + 46,1991 - 20\log_{10}|H1(s)H2(s)H3(s)| \tag{25a}$$

$$Error3_{phase} = Phase_{Ld(s)} - Arg(H1(s)H2(s)H3(s)) \tag{25b}$$

We note that the magnitude of the operational inductance $|Ld(s)| = -46,1991\,\text{dB}$ for $f = 0.001\,\text{Hz}$. The curve giving the evolution of the magnitude and the phase of the Error3 versus frequency is represented in Figure 7(c).

We note that the frequency $Fce = 200\,\text{Hz}$ corresponds to the last minimum phase $\varphi_{\min} = -4.56$ degree, so $\beta = 1.1727$, $Td''''(\text{sec}) = 0.0007352$, $Td0''''(\text{sec}) = 0.0008622$.

We conclude that there are no peaks of phase; therefore, output of the process and the optimal model we have adopted is of the fourth order.

The operational inductance with the initial estimate time constants can be written as:

$$Ld(s) = 0.004898\frac{(1 + 0.941527s)\,(1 + 0.111834s)\,(1 + 0.0047025s)\,(1 + 0.0007352s)}{(1 + 4.207969s)\,(1 + 0.134168s)\,(1 + 0.0055991s)\,(1 + 0.0008622s)} \tag{26}$$

Figure 8 shows the initial residual representing the difference between the operational inductance frequency response giving by (26) and the experimental one. The error in the phase varies between -0.2513 and 1.589 degrees, while the error in the magnitude is within the range of 0–0.7165 dB.

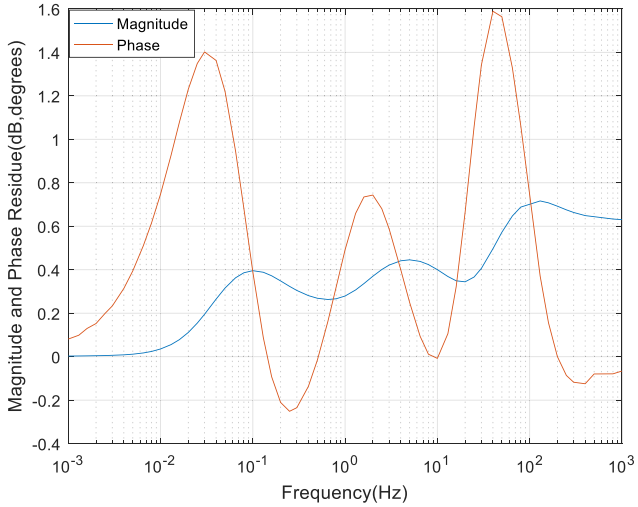

Figure 8. Variation of the operational inductance Residue versus Frequency.

7. OPTIMIZATION OF THE TIME CONSTANTS

When identifying the time constants of operational inductance of synchronous machine, we find that many researchers [31, 32] consider only the error in the magnitude, whereas the other researchers [33]

have used a weighting function containing both the magnitude and phase. Another study shows that the errors resulting from both the magnitude and phase can be used in different manners in determining the best values of time constants [34].

An optimization method will be presented in this study. This consists in taking the differential of the magnitude with respect to the frequency. The real data will also be used as input for the optimization process.

7.1. Optimization of Time Constants by Differentiation

The variables used in this process are frequency, magnitude, and phase of the real data. We started by taking the difference between the 1st and 2nd data points of magnitude and so on. The same process is repeated for phase and frequency data, then we divide the difference in magnitude by the difference in frequency. Finally, we obtain the slope of the magnitude with respect to the frequency.

So the new data becomes: ΔM, ΔF, $\Delta\varphi$ and slope, where:

- $\Delta M1 = M2 - M1$; $\Delta M2 = M3 - M2 \ldots etc.$
- $\Delta F1 = F2 - F1$; $\Delta F2 = F2 - F1 \ldots etc.$
- $\Delta\varphi1 = \varphi2 - \varphi1$; $\Delta\varphi2 = \varphi3 - \varphi2 \ldots etc.$
- $slope1 = \frac{\Delta M1}{\Delta F1}$; $slope2 = \frac{\Delta M2}{\Delta F2} \ldots etc.$

From the new data, we need to calculate the average value of two successive frequencies. This process is repeated for different values of the frequencies.

$$F_{avg1} = \frac{F1 + F2}{2}; \quad F_{avg2} = \frac{F2 + F3}{2} \ldots etc.$$

We now have new variables available for the optimisation process. The two most important variables we need to consider are $\frac{\Delta M}{\Delta F}$ and F_{avg}.

7.2. Configuring Data for Optimization

After determining the variables, the optimization process will begin, and the results of the simulations and discussions will be made, according to the following steps:

Step 1: we consider the frequency variation:

$$\Delta F1 = F2 - F1; \quad \Delta F2 = F2 - F1 \ldots etc.$$

The variables $\frac{\Delta M}{\Delta F}$, $\frac{\Delta\varphi}{\Delta F}$ against average frequency are presented in Figure 9.
The curve of Figure 9(a) is almost similar to that of Figure 5. However, for the first figure, the maximum slope of the magnitude and the minimum phase are obtained for $Fce = 0.035\,\text{Hz}$ (Figure 9(a)) against $0.08\,\text{Hz}$ (Figure 5) as illustrated in the second figure. In order to obtain the same shape and frequency for both figures, and since the x-axis is in logarithmic scale, we introduce the logarithmic scale.

Step 2: We define actually the variable ΔF with a new form:

$$\Delta F1 = \log_{10}(F2) - \log_{10}(F1); \quad \Delta F2 = \log_{10}(F3) - \log_{10}(F2) \ldots etc.$$

The result so obtained is presented in Figure 10(a). The shape of the latter totally coincides with the desired curve of Figure 5. The maximum slope is set at a frequency of $0.09\,\text{Hz}$. Thus, the objective of this study has been achieved.

7.3. Discussions on the Simulations

From the simulation, we note that Figure 10(a) gives the desired curve which is characterized by a maximum at the frequency $0.09\,\text{Hz}$. This curve is important because it defines the minimum phase of the desired curve. Through this analysis, it can be affirmed that the use of the differential magnitude data gives the value of Fce by using the average value of two points, compared to the data of the phase basing on the choice of only one frequency.

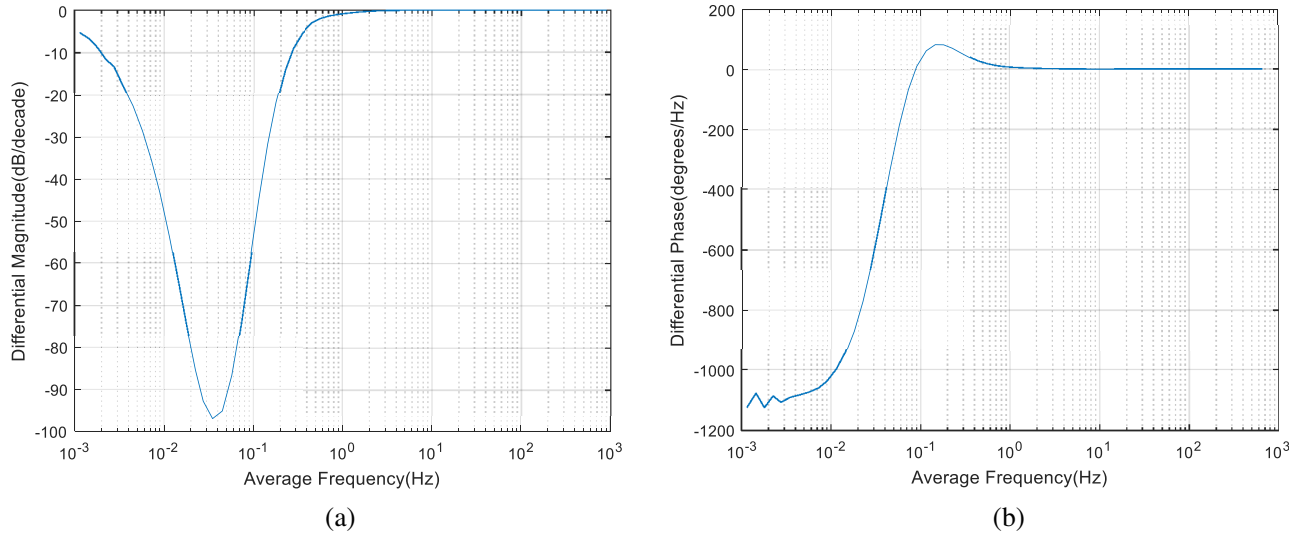

(a) (b)

Figure 9. (a) Variation of differential magnitude against average frequency. (b) Variation of differential phase against average frequency.

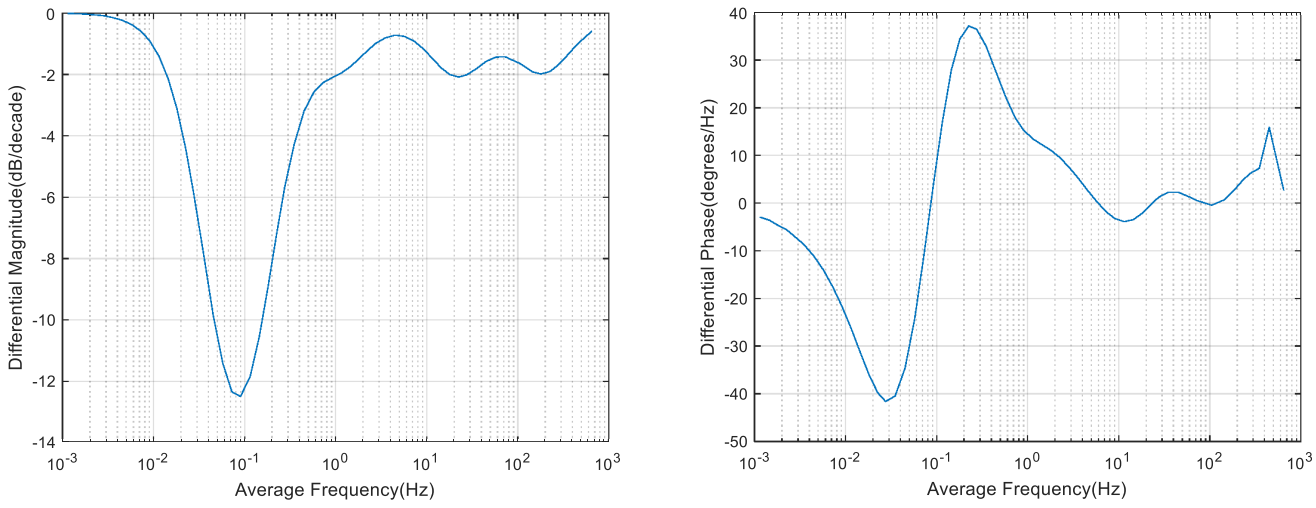

(a) (b)

Figure 10. (a) Variation of operational inductance differential magnitude (slope) against average frequency. (b) Variation of operational inductance differential phase against average frequency.

7.4. Calculating the Frequency Response

This step is important in the optimization process because it explains how to obtain the frequency response from the differential magnitude data. Equations (18) and (19) will be used here:

Also, we have:

$$Tf(s) = \frac{(1 + sTd)}{(1 + sTd0)} \tag{27}$$

where $Tf(s)$ is the transfer function to calculate the frequency response, by varying the frequency from 0 Hz to 100 Hz. To determine the relationship between the slope of the magnitude, the frequency curve and β, we calculate frequency responses for eight values of β in the range [1.1, 5.5]. Note that the center frequency has been taken equal to 1 Hz.

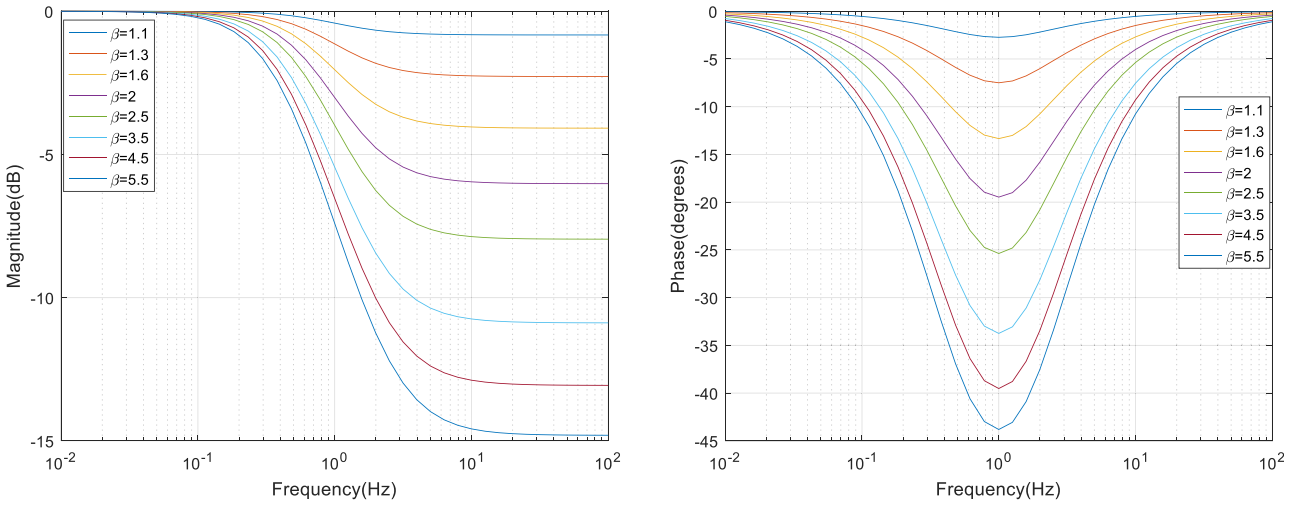

(a) (b)

Figure 11. (a) Variation of magnitude against frequency. (b) Variation of phase against frequency.

Figure 11 represents the variation of the magnitude and phase according to the frequency. We notice that the maximum of the slope and the minimum of the phase are located at the center frequency of 1 Hz.

The next step aims to determine the slope of each of the curves, from the frequency responses.

7.5. Slope Determination

The three points, frequency $Fc = 1\,\text{Hz}$ for different values of β (see Figure 11(a)), with the frequencies $F1$ just below and $F2$ just above, should be used to determine the slope.

We have:

$$\begin{aligned} \Delta F1 = F1 - Fc; \quad & \Delta F2 = Fc - F2 \\ \Delta M1 = M1 - Mc; \quad & \Delta M2 = Mc - M2 \\ slope1 = \tfrac{\Delta M1}{\Delta F1}; \quad & slope2 = \tfrac{\Delta M2}{\Delta F2} \end{aligned}$$

We take the average value of the slopes:

$$slope = \frac{slop1 + slope2}{2}$$

Figure 12 represents the variation of the slope in (dB/Hz) as a function of β.

According to this curve, we notice that the slope increases pseudo-linearly with β. However, the scale of the slope should be changed. In accordance with the Bode diagram, the slope of the magnitude is expressed in terms of dB/decade. This allows obtaining the graph shown in Figure 13.

The variation of the maximum slope in (dB/decade) as a function of β is given by the following function:

$$slope = 20\frac{(\beta - 1)}{(\beta + 1)} \tag{28}$$

7.6. Determination of the Optimum Time Constant

The curve in Figure 13 is essential to determining the optimal time constants which depend on β according to Equations (18) and (19). In fact, Figure 10(a) permits obtaining the various maxima slopes found for different frequencies Fce. The corresponding values of β are deduced from Figure 13. The time constants are summarized in Table 1.

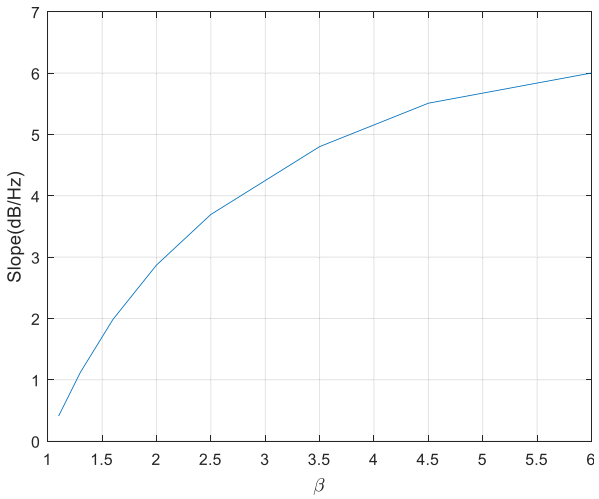

Figure 12. Variation of slope in (dB/Hz) against β.

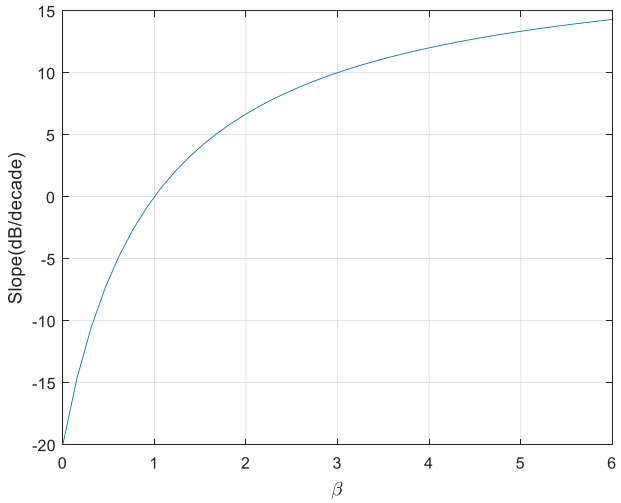

Figure 13. Variation of slope in (dB/decade) against β.

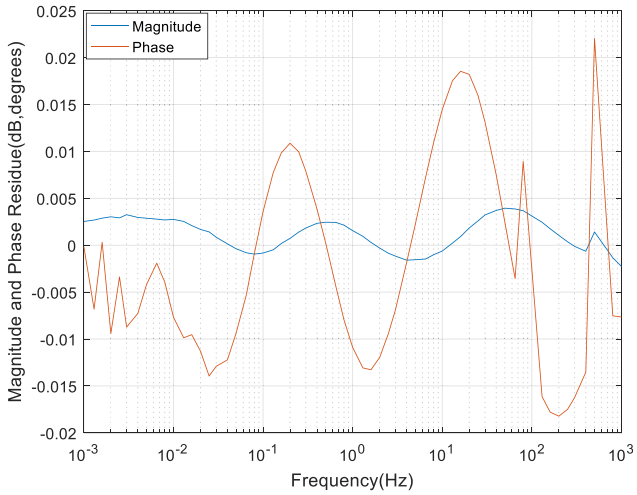

Figure 14. Variation of the operational inductance Residue versus frequency (after optimization).

Table 1. Estimation of optimal time constants.

Slope (dB/decade)	12.5	1.958	2.086	1.986
β	3.9394	1.1343	1.3698	1.0768
Fce (Hz)	0.09	1.15	22.5	180
Td (sec)	$Td0' = 3.950662$	$Td0'' = 0.147473$	$Td0''' = 0.008286$	$Td0'''' = 0.000918$
Td (sec)	$Td' = 0.908283$	$Td'' = 0.126934$	Td'''(sec) $= 0.006788$	$Td'''' = 0.000760$

7.7. Comparison of Results

The residue shown in Figure 14 represents the error between the frequency responses of the analytical method after optimization and the measured of operational inductance. We show that the error in the phase varies between -0.01822 and 0.02204 degrees, while the error varies between -0.002262 and 0.003836 dB in the magnitude.

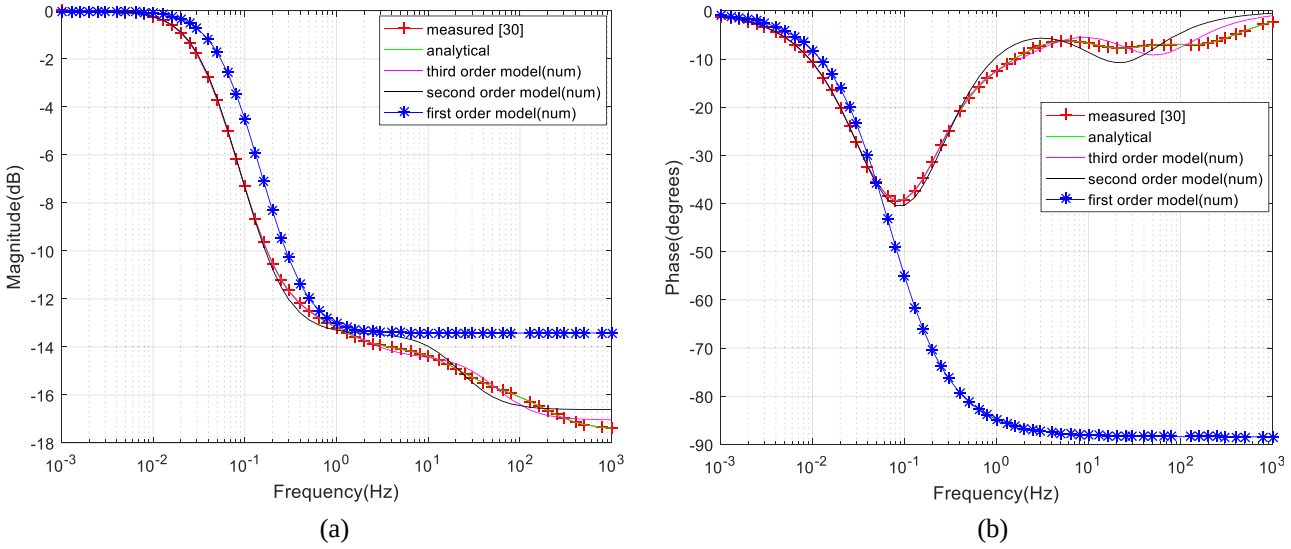

Figure 15. (a) Operational inductance magnitude versus frequency. (b) Operational inductance phase versus frequency.

We note that the introduction of the optimization process has improved the time constants significantly, and the error becomes minimum.

Figure 15 shows the frequency responses of the different operational inductances, namely the measured [30], analytical, and finally numerical ones. The numerical operational inductances have been obtained according to first order, second order, and third order models.

We observe a satisfactory agreement between the measured curve and analytical one. Concerning the numerical method for the 3rd order model, we note a slight disagreement for the magnitude in the frequency range between 80 and 1000 Hz. For the phase, it is seen that a clear difference appears in the range of 8 to 1000 Hz. For the second order model we see a slight difference in magnitude and phase compared to the tests. Then for the first order model we notice a significant difference in the magnitude and phase in the range of 0.006 to 1000 Hz.

8. CONCLUSION

In this paper, we use an analytical method to estimate the time constants of the synchronous machine from Standstill Frequency Response Testing. This method is based on the standard theory of linear systems to locate the values of poles and zeros in the frequency response and determines the optimal order of the equivalent circuit which can model the machine accurately. It also allows to use the values of the initial time constants as an initial vector for numerical methods. We have also shown the importance of the precision of the value of the stator resistance on the determination of the time constants. The comparison of initial residue with the obtained after the optimisation process shows clearly that the procedure based on the optimisation of parameters by differentiation allows obtaining optimal time constants. Such comparison demonstrates the effectiveness of the method optimisation.

REFERENCES

1. Aghamohammadi, M. R., A. Beik Khormizi, and M. Rezaee, "Effect of generator parameters inaccuracy on transient stability performance," *Power and Energy Engineering Conference (APPEEC)*, 1–5, Mar. 2010.
2. Ghomi, M. and Y. N. Sarem, "Review of synchronous generator parameters estimation and model identification," *2007 42nd International Universities Power Engineering Conference*, 228–235, 2007.

3. Kamwa, I., M. Pilote, H. Carle, P. Viarouge, B. Mpanda-Mabwe, and M. Crappe, "Computer software to automate the graphical analysis of sudden-short-circuit oscillograms of large synchronous machines," *IEEE Trans. Energy Convers.*, Vol. 10, No. 3, 399–406, Sep. 1995.
4. Kamwa, I., P. Viarouge, and R. Mahfoudi, "Phenomenological models of large synchronous machines from short-circuit tests during commissioning-a classical/modern approach," *IEEE Trans. Energy Convers.*, Vol. 9, No. 1, 85–97, Mar. 1994.
5. "IEEE guide for test procedures for synchronous machines part iacceptance and performance testing Part II. Test procedures and parameter determination for dynamic analysis," *IEEE Std 115-2009 Revis. IEEE Std 115-1995*, 1–219, May 2010.
6. Sellschopp, F. S. and M. A. Arjona, "DC decay test for estimating d-axis synchronous machine parameters: A two-transfer-function approach," *IEE Proc. — Electr. Power Appl.*, Vol. 153, No. 1, 123–128, Jan. 2006.
7. Sellschopp, F. S. and M. A. Arjona, "Semi-analytical method for determining d-axis synchronous generator parameters using the dc step voltage test," *IEE Proc. — Electr. Power Appl.*, Vol. 1, No. 3, 348–354, May 2007.
8. Maurer, F., T. Xuan, and J. Simond, "Tow full parameter identification methods for synchronous machine applying DC-decays tests for a rotor in arbitrary position," *IEEE Transactions on Industry Applications*, Vol. 53, No. 4, 3505–3518, Jul.–Aug. 2017.
9. Wamkeue, R., C. Jolette, and I. Kamwa, "Advanced modeling of a synchronous generator under line-switching and load-rejection tests for isolated grid applications," *IEEE Trans. Energy Convers.*, Vol. 25, No. 3, 680–689, Sep. 2010.
10. Hiramatsu, D., M. Kakiuchi, K. Nagakura, Y. Uemura, K. Koyanagi, K. Hirayama, S. Nagano, R. Nagura, and K. Nagasaka, "Analytical study on generator load rejection characteristic using advanced equivalent circuit," *2006 IEEE Power Engineering Society General Meeting*, 18–22, Montreal, QC, Jun. 2006.
11. Melgoza, J. J. R., G. T. Heydt, A. Keyhani, B. L. Agrawal, and D. Selin, "An algebraic approach for identifying operating point dependent parameters of synchronous machines using orthogonal series expansions," *IEEE Trans. Energy Convers.*, Vol. 16, No. 1, 92–98, Mar. 2001.
12. Melgoza, J. J. R., G. T. Heydt, A. Keyhani, B. L. Agrawal, and D. Selin, "Synchronous machine parameter estimation using the Hartley series," *IEEE Trans. Energy Convers.*, Vol. 16, No. 1, 49–54, Mar. 2001.
13. Rengifo, C. F., C. Girón, J. Palechor, A. Diego, and M. Bravo, "Identification of a synchronous generator parameters using recursive least squares and kalman filter," *20 Revista Ciencia en Desarrollo*, Vol. 12, No. 1, 13–21, Jan.–Jun. 2021.
14. Shariati, O., A. A. M. Zin, and M. R. Aghamohammadi, "Application of neural network observer for on-line estimation of salient-pole synchronous generator's dynamic parameters using the operating data," *2011 4th International Conference on Modeling, Simulation and Applied Optimization (ICMSAO)*, 1–9, 2011.
15. Henrique, L., D. Kornrumpf, and S. I. Nabeta, "Deterination of synchronous parameters through the SSFR test and artificial neural networks," *The 9th International Conference on Power Electronics, Machines and Drives (PMD 2018)*, 2018.
16. Fard, R. D., M. Karrari, and O. P. Malik, "Synchronous generator model identification using Volterra series," *IEEE Power Engineering Society General Meeting*, Vol. 2, 1344–1349, 2004.
17. Sen, S. K. and B. Adkins, "The application of the frequency response method to electrical machines," *Proc. IEE*, Vol. 103, No. 4, 378–391, 1956.
18. Belqorchi, A., U. Karragac, J. Mehseredjian, and I. Kamwa, "Standstill frequency response test and validation of a large Hy-drogenerator," *IEEE Transactions on Power Systems*, Vol. 34, No. 3, 2261–2269, May 2019, ISSN: 0885-8950, DOI: 10.1109/TPWRS.2018.2889510.
19. Sellschopp, F. S. and M. A. Arjona, "Determination of synchronous machine parameters using standstill frequency response tests at different excitation levels," *2007 IEEE International Electric Machines & Drives Conference*, Vol. 2, 1014–1019, 2007.

20. Kutt, F., S. Racewicz, and M. Michna, "SSFR test of synchronous machine for different saturation levels using finite-element method," *IECON 2014 — 40th Annual Conference of the IEEE Industrial Electronics Society*, 907–911, 2014.
21. Radjeai, H., A. Barakat, S. Tnani, and G. Champenois, "Identification of synchronous machine by Standstill Frequency Response (SSFR) method influence of the stator resistance," *2010 XIX International Conference on Electrical Machines (ICEM)*, 1–5, 2010.
22. "IEEE guide for synchronous generator modeling practices and applications in power system stability analyses," *IEEE Std 1110-2002 Revis. IEEE Std 1110-1991*, 1–72, 2003.
23. Dandeno, P. L. and A. T. Poray, "Development of detailed turbogenerator equivalent circuits from standstill frequency response measurements," *IEEE Trans. Power Appar. Syst.*, Vol. 100, No. 4, 1646–1655, Apr. 1981.
24. Hernandez-Anaya, O., T. Niewierowicz, E. Campero-Littlewood, and R. Escarela-Perez, "Noise impact in the determination of synchronous machine equivalent circuits using SSFR data," *2006 3rd International Conference on Electrical and Electronics Engineering*, 1–4, 2006.
25. Firouzi, B. B., E. Jamshidpour, and T. Niknam, "A new method for estimation of large synchronous generator parameters by genetic algorithm," *World Applied Sciences Journal*, Vol. 4, No. 3, 326–331, 2008.
26. Srinivasan, G. K. and H. T. Srinivasan, "In situ parameter estimation of synchronous machines using genetic algorithm method," *Advances in Electrical and Electronic Engineering*, Vol. 14, No. 3, 254–266, 2016, DOI: 10.15598/aeee.v14i3.1707.
27. Bendaoud, E., H. Radjeai, and O. Boutalbi, "Parameters identification of synchronous machine based on particle swarm optimization," *The International Conference on Energy and Green Computing (ICEGC'2021)*, Vol. 336, 00052, 2022.
28. Bendaoud, E., H. Radjeai, and O. Boutalbi, "Identification of nonlinear synchronous generator parameters using stochastic fractal search algorithm," *Journal of Control, Automation and Electrical Systems*, Vol. 32, 1639–1651, 2021.
29. Krause, P. C., "Operational impedances and time constants of synchronous machines" *Analysis of Electric Machinery*, 271–297, McGraw-Hill, 1986.
30. Electric Power Research Institute, "Compendium of the EPRI Workshop on determination of synchronous machine stability study constants," by N. E. I Parsons, Aug. 1980.
31. Niewierowicz, T., R. Escarela-Perez, and E. Campero-Littlewood, "Hybrid genetic algorithm for the identification of high-order synchronous machine two-axis equivalent circuits," *Computers and Electrical Engineering*, Vol. 29, 5055–22, 2003.
32. Kano, T., H. Nakayama, T. Ara, and T. Matsumura, "A calculation method of equivalent circuits constants with mutual leakage reactance on synchronous machine with damper winding," *IEEJ 2007*, Vol. 127-D, No. 7, 761–766, 2007.
33. Pao-la-or, P., T. Kulworawanichpong, and A. Oonsivilai, "Frequency domain parameter estimation of a synchronous generator using bi-objective genetic algorithms," *Proceeding of the 7th WSEAS International Conference on Simulation, Modeling and Optimisation*, 429–433, Beijing, China, Sep. 2007.
34. Walton, A., "A systematic method for the determination of the parameters of synchronous machines from the results of frequency response tests," *IEEE Trans. Energy Convers.*, Vol. 15, No. 2, 218–223, Jun. 2000.